

Changes in Koppen–Trewartha climate classification over South America from RegCM4 projections

Julio P. R. Fernandez,^{1*} Sergio H. Franchito,¹ V. Brahmananda Rao¹ and Marta Llopart²

¹Centro de Previsão de Tempo e Estudos Climáticos, CPTEC, Instituto Nacional de Pesquisas Espaciais, INPE, São José dos Campos, SP, Brazil

²Departamento de Física, Centro de Meteorologia de Bauru (IPMet), Universidade Estadual Paulista (UNESP), São Paulo, Brazil

*Correspondence to:

J. P. R. Fernandez, Centro de
Previsão de Tempo e Estudos
Climáticos, CPTEC, Instituto
Nacional de Pesquisas Espaciais,
INPE, C.P. 515, 12245-970, São
José dos Campos, SP, Brazil.
E-mail:
pablo.reyes@cptec.inpe.br

Abstract

The Koppen–Trewartha (K–T) classification is used to investigate the biomes change in the future climate over South America (SA). For the middle (2035–2060) and end (2075–2100) of the 21st century mean ensemble of Regional Climate Model version 4 simulations for the Representative Concentration Pathway 8.5 scenario are presented. The global-coupled models of Coupled Model Intercomparison Project Phase 5 drive the members for the period 1970–2100 using different physics configurations. The delta change approach is applied to filter out the bias of the model simulation. Notable changes of the K–T climates are found in SA, mainly in Brazil. Replacement of tropical wet-dry (Aw) by dry semiarid (Bs) occurs over Northeast Brazil (NEB). Reduction of tropical humid (Ar) and an increase of Aw is projected in the North Brazil and Amazon. Retreat of subtropical humid (Cr) replaced by Aw is found in the Southeast Brazil. An increase of subtropical winter-dry (Cw) and decrease Cr is noted in Argentina and in Paraguay Cr is replaced by Ar. In the south of SA, a retreat of subarctic oceanic (Eo) and an increase of temperate oceanic (Do) and dry arid (Bw) occur. In general, the projected changes of K–T climate types in the 21st century over SA show a tendency for a drier climate.

Keywords: climate classification; regional climate change; South America

Received: 7 December 2016
Revised: 3 May 2017
Accepted: 15 September 2017

1. Introduction

Koppen–Trewartha (K–T) climate classification (Trewartha and Horn, 1980) has been applied to outputs of Regional Climate Models (RCMs) to study the impact of climate change on the biomes distribution in many regions of the Northern Hemisphere (Castro *et al.*, 2007; Gao and Giorgi, 2008; Gallardo *et al.*, 2013; Chan *et al.*, 2016). For the South America (SA) region a few studies haven made. SA presents in the north–south extension features of tropical, subtropical and extratropical climates. Due to the presence of two large oceans (the Pacific and the Atlantic), the Andes Cordillera and different biomes, such as the Amazon forest, desert and arid regions in northern Chile and Northeast Brazil (NEB), respectively, numerous dynamical and physical processes act in the continent, which results in a variety of climates (Garreaud *et al.*, 2009). Recently, Gallardo *et al.* (2016) applied K–T climate classification to RCM simulations in the frame of CLARIS-LPB EU project driven by the Special Report on Emission Scenarios (SRES) A1B scenario (Nakićenović *et al.*, 2000). They found that important climate changes may occur in 27% of SA at the end of 21st century. Also, transitions for drier climates may happen particularly over Brazil.

In the present paper, we show the projected alterations in the K–T climate types over SA in the 21st century from the mean ensemble Regional Climate Model version 4 (RegCM4) simulations under the

Representative Concentration Pathway (RCP) 8.5 scenario. Differently from Gallardo *et al.* (2016), who used CMIP3 data, in the present study Coupled Model Intercomparison Project Phase 5 (CMIP5) models drive the members for the period 1970–2100 using different physics configurations. We use the Coordinated Regional Downscaling Experiment (CORDEX) RegCM4 hyper-Matrix (CREMA) data for SA (Giorgi, 2014) whose objective is to reduce different sources of uncertainty associated with driving Atmospheric–Oceanic General Circulation Models (AOGCMs), the greenhouse gas RCPs, and model physics configuration. To our knowledge, this is the highest ensemble with RegCM4 for the SA using CMIP5 data. Section 2 shows a short description of the model and simulations design, as well as the K–T climate classification. The simulations for the present climate and future projected changes are shown in Section 3, and conclusions are presented in Section 4.

2. Model description and simulations design

The simulations used in the study are conducted by the Abdus Salam International Center for Theoretical Physics (ICTP) using RegCM4 (Giorgi *et al.*, 2012). The model domain covers entire SA, following the CORDEX protocol (Giorgi *et al.*, 2009) with a grid spacing of 50 km (Figure 1). The four RegCM4 members (Table S1, Supporting information) from CREMA

using different physical configurations (surface processes and cumulus convection) and forcing at the lateral boundaries (AOGCMs) are described in Giorgi (2014). The period of all simulations is 1970–2100 (continuous run). In this study, we used the ensemble mean from the RegCM4 simulations, averaged over SA, for three time slices: the present-day climate (1975–2000) and two future time slices for the middle (2035–2060) and end (2075–2100) of the 21st century. The historical greenhouse gases, aerosols, and natural forcings are used, until 2005 and projections from RCP 8.5 scenario after.

To identify different types of climate regimes, we use the K–T climate classification (Trewartha and Horn, 1980). It has been used to describe the potential distribution of natural vegetation based on climatic thresholds (Lohmann *et al.*, 1993). It builds on a combination of average annual, monthly, and seasonal averages of the surface air temperature and precipitation. Six climate regimes are identified, each containing many types. Table 1 shows K–T climate classification and their correspondence with the natural vegetation type.

In general, the simulations over SA show biases that affect the climatic indices. The values of K–T calculated show high sensibility to thresholds so that the reasonable characterization of climate types from simulations is difficult. In the present study, we use a simple method to overcome this problem. In this approach, the climate signal is obtained by subtracting the long-term monthly mean of the temperature of the present climate from the future projection, so that the model error has been canceled (Mahlstein *et al.*, 2013; Feng *et al.*, 2014). Then this signal is added to long-term monthly mean observational data to obtain the future climate projection. Different from the temperature, in the case of precipitation a ratio between the future climate projection and the reference is obtained. Then, this ratio is multiplied by the observed data. This delta method is commonly used in climate change studies for the analysis of future changes of Köppen climate zones (Gao and Giorgi, 2008; Mahlstein *et al.*, 2013; Feng *et al.*, 2014; Belda *et al.*, 2016; and many others).

However, the method has some drawbacks. The transient climate changes, as well as the changes in the interannual and diurnal climatic variability, are not represented. The use of bias correction in the model outputs may be an alternative (Piani *et al.*, 2010), but its application may modify the sign of climate change both of temperature and precipitation so that for some regions the impact on the signal may be higher, adding more a factor of uncertainty of the projections (Piani *et al.*, 2010; Boberg and Christensen, 2012; Christensen and Boberg, 2012; Solman, 2016).

To assess and correct the projections the precipitation and surface air temperature monthly mean data from Climate Research Unit (CRU; Harris *et al.*, 2014) are used to obtain the K–T classification types. Comparison between CRU and University of Delaware (UDEL; Matsuura and Willmott, 2011) data for SA shows that the differences are smaller for temperature, but the

Table 1. The Köppen–Trewartha (K–T) climate classification (Trewartha and Horn, 1980) and their correspondence with natural landscapes (adapted from Castro *et al.*, 2007).

Climate	K–T	Prevalent native vegetation type
Tropical humid	Ar	Rain Forest
Tropical wet-dry	Aw	Savanna
Dry arid	Bw	Desert
Dry semiarid	Bs	Steppe
Subtropical summer-dry	Cs	Hardleaved evergreen trees and shrubs
Subtropical summer-wet	Cw	Woodland patches, shrubs and prairies
Subtropical humid	Cr	Longleaf trees, slash pines and deciduous forest in inland areas
Temperate oceanic	Do	Dense coniferous forest with large trees
Temperate continental	Dc	Needleleaf and deciduous tall broadleaf forest
Subarctic oceanic	Eo	Needleleaf forest
Subarctic continental	Ec	Tayga
Tundra	Ft	Tundra
Ice cap	Fi	Permanent ice cover

where, Ar: All months above 18 °C and less than 3 dry months (1); Aw: Same as Ar, but 3 or more dry months; Bw: Annual precipitation P (in cm) smaller or equal than $0.5 \cdot A$ (2); Bs: Annual precipitation P (in cm) greater than $0.5 \cdot A$; Cs: 8–12 months above 10 °C, annual rainfall less than 89 cm and dry summer (3); Cw: Same thermal criteria as Cs, but dry winter (4); Cr: Same as Cw, with no dry season; Do: 4–7 months above 10 °C and coldest month above 0 °C; Dc: 4–7 months above 10 °C and coldest month below 0 °C; Eo: Up to 3 months above 10 °C and temperature of the coldest month above –10 °C; Ec: Up to 3 months above 10 °C and the coldest month below or equal to –10 °C; Ft: All months below 10 °C; Fi: All months below 0 °C.

- (1) Dry month: Less than 6 cm monthly precipitation.
- (2) $A = 2.3T - 0.64P_w + 41$, being T the mean annual temperature (in °C) and P_w the percentage of annual precipitation occurring in the coolest 6 months.
- (3) Dry summer: The driest summer month less than 3 cm precipitation and less than one-third of the amount in the wettest winter month.
- (4) Dry winter: Precipitation in the wettest summer month higher than 10 times that of the driest winter month.

datasets show important differences for precipitation in some regions (Solman *et al.*, 2013). This is associated to use a different number of gauges, methods of quality control and spatial interpolation. It must be taken into account that in mountainous regions and little quantity of data the uncertainty is higher. However, as it will be shown the impact of the choice of the datasets on the evaluation of model projections is negligible.

3. Present climate and future changes

Figures 2(a) and (b) show the comparison of the distribution of K–T climate types over SA calculated from observations and the present-day mean ensemble simulations of the model (1975–2000), respectively. Figure 2(a) shows that the dominant climate types over SA are A-tropical, B-dry, and C-subtropical. In the Andes region and south of the continent Dc, Ec, and tundra (Ft) are dominant. As seen in Figure 2(b), the mean ensemble simulation reproduces reasonably well the distribution of K–T climates over SA, mainly in

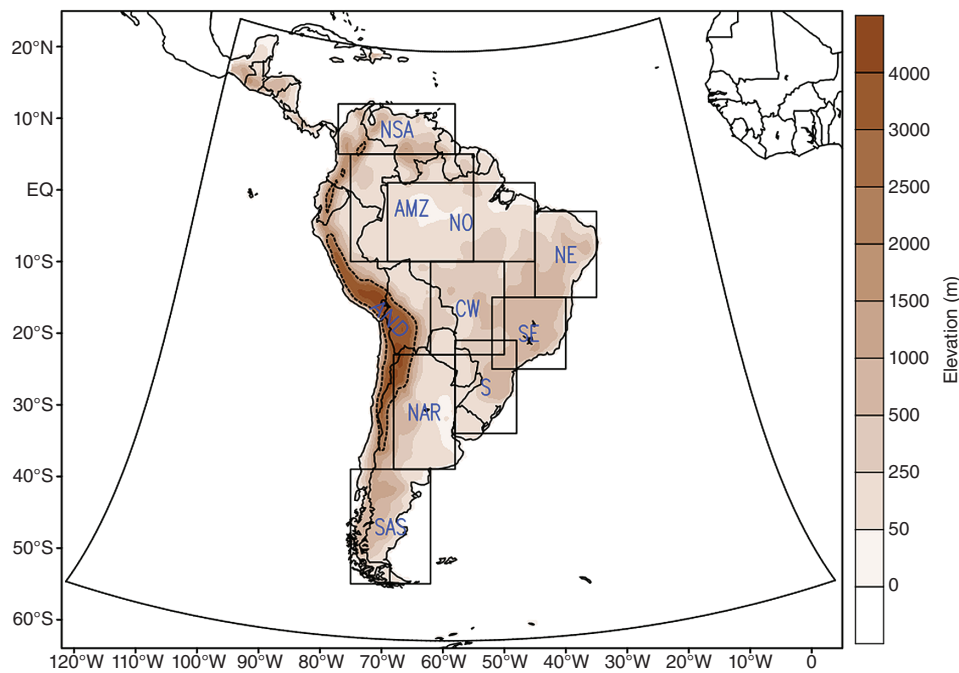


Figure 1. Model domain. Shown are the topography (m) and regions of SA: NSA: North of South America, 5° – 12° N, 77° – 58° W; AMZ: Amazon, 10° S– 5° N, 75° – 55° W; NAR: North of Argentina, 39° – 23° N, 68° – 58° W; SSA: South of South America, 55° – 39° S, 75° – 62° W; AND: Andes 2000 m above msl, and over Brazil: NO: north, 10° S– 1° N, 69° – 45° W; CW: center-west, 23° – 10° S, 62° – 50° W; NEB: northeast, 15° – 3° S, 45° – 35° W; SE: southeast, 25° – 15° S, 52° – 40° W; and S: south, 34° – 21° S, 58° – 48° W.

the tropical region. The main differences occur in NEB (Aw instead of Bs) and Southeast Brazil (Cr instead of Aw), south of Argentina and mountain areas (Cr instead of Bs). These differences can be attributed to the over/underestimation of the precipitation in these zones (wet/dry bias) and also to the positive/negative bias in the surface air temperature (cold/warm bias) simulated by the model. The validation and discussion on the bias of the RegCM4 simulations for the present-day climate can be seen in Coppola *et al.* (2014). In general, the RegCM4 captures the main patterns of the observed precipitation and surface air temperature for SA. The use of K–T classification in global and regional models driven by coupled models of CMIP5 show similar results (Teichmann *et al.*, 2013; Feng *et al.*, 2014). K–T climates from the projected simulations with uncorrected data are shown in Figure 3. The present-day model bias affects the future climate classification showing warmer climates.

K–T types distribution for the middle (2035–2060) and end (2075–2100) of the 21st century using CRU data to correct the simulations are presented in Figures 2(c) and (d). Comparing with Figure 2(a) changes of the K–T climate types distribution in NEB, North Brazil, Amazon, Southeast Brazil, and Center-West of Brazil are seen in the mid-21st century (Figure 2(c)). Over NEB the tropical wet-dry climate, Aw (savanna), is replaced by a drier climate of Bs (steppe). Over North Brazil and Amazon, there is a reduction of Ar (rain forest) and an increase of Aw (savanna). A retreat of Cr (subtropical humid climate) replaced by Aw (tropical wet-dry climate) is found in the Southeast Brazil, suggesting the change of longleaf

trees by savanna. In some parts of the South Brazil, there is a reduction of Cr and an increase of Ar. Further changes can be seen in Paraguay, Argentina, and the eastern SA. Over Paraguay there is a decrease of Cr, subtropical humid climate, which is substituted by Aw, indicating the change of longleaf trees by savanna. An increase of Cw and decrease of Cr climates are noted in Argentina, showing an expansion of the woodland and reduction of longleaf trees in the region. In the western SA, there is an increase of Bs climate in Bolivia and in the west coast an increase of Bw is found. In the south of SA, a retreat of Eo and an increase of Do and Bw are noted.

It can be seen from Figures 2(a) and S1(a) that the K–T climate types derived from CRU and UDEL data show small differences. However, when the CRU data has used the distribution of K–T climates is smoother. This is because the different interpolation method in the two datasets.

The projected changes in the temperature and precipitation are responsible for the K–T climate transitions. To examine the relative roles of the changes in the temperature and precipitation K–T climate types are calculated considering the individual changes in these variables, i.e. using the delta in temperature with the observed precipitation and vice versa. The K–T climate classification in these two cases and the K–T climate transitions are presented in Figures 4(a) and (b) and Figures 4(c) and (d), respectively. As can be seen in Figures 2(e) and (f) many transitions projected in future (2075–2100) are reproduced in the regions SE, S, and mountainous regions of SA (mainly in middle latitudes) if the precipitation is held constant (Figures 4(a) and

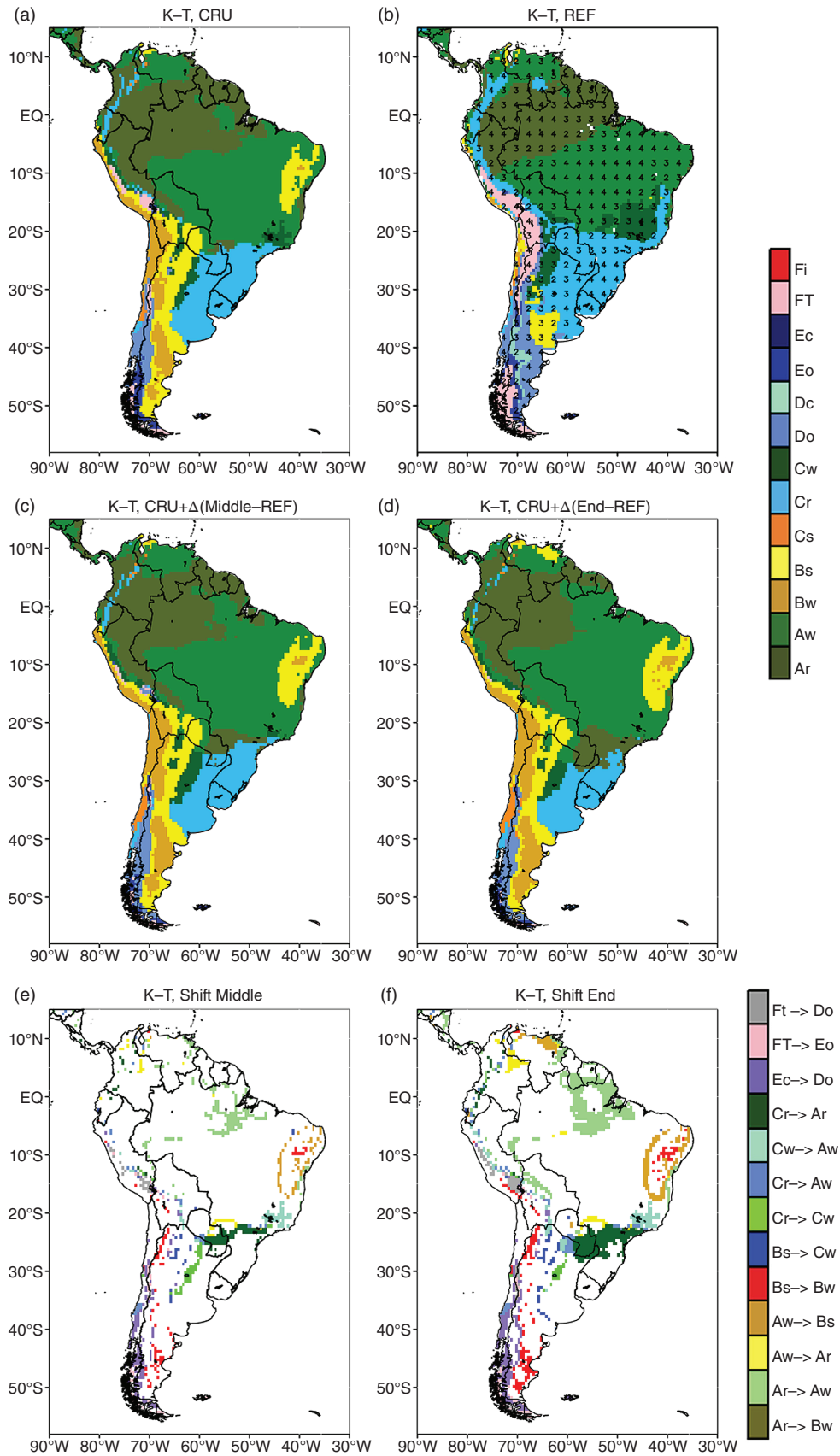


Figure 2. Koppen–Trewartha (K–T) climate types over SA calculated from (a) CRU observations; (b) RegCM4 mean ensemble for the present-day climate (1975–2000); CRU observations plus delta climate changes for (c) middle (2035–2060) and (d) end (2075–2100) of the 21st century. Projected major K–T climate types transitions for (e) middle (2035–2060) and (f) end (2075–2100) of the 21st century under RCP 8.5 scenario. The numbers in the panel (b) indicate how many members have the same climate types as the mean ensemble.

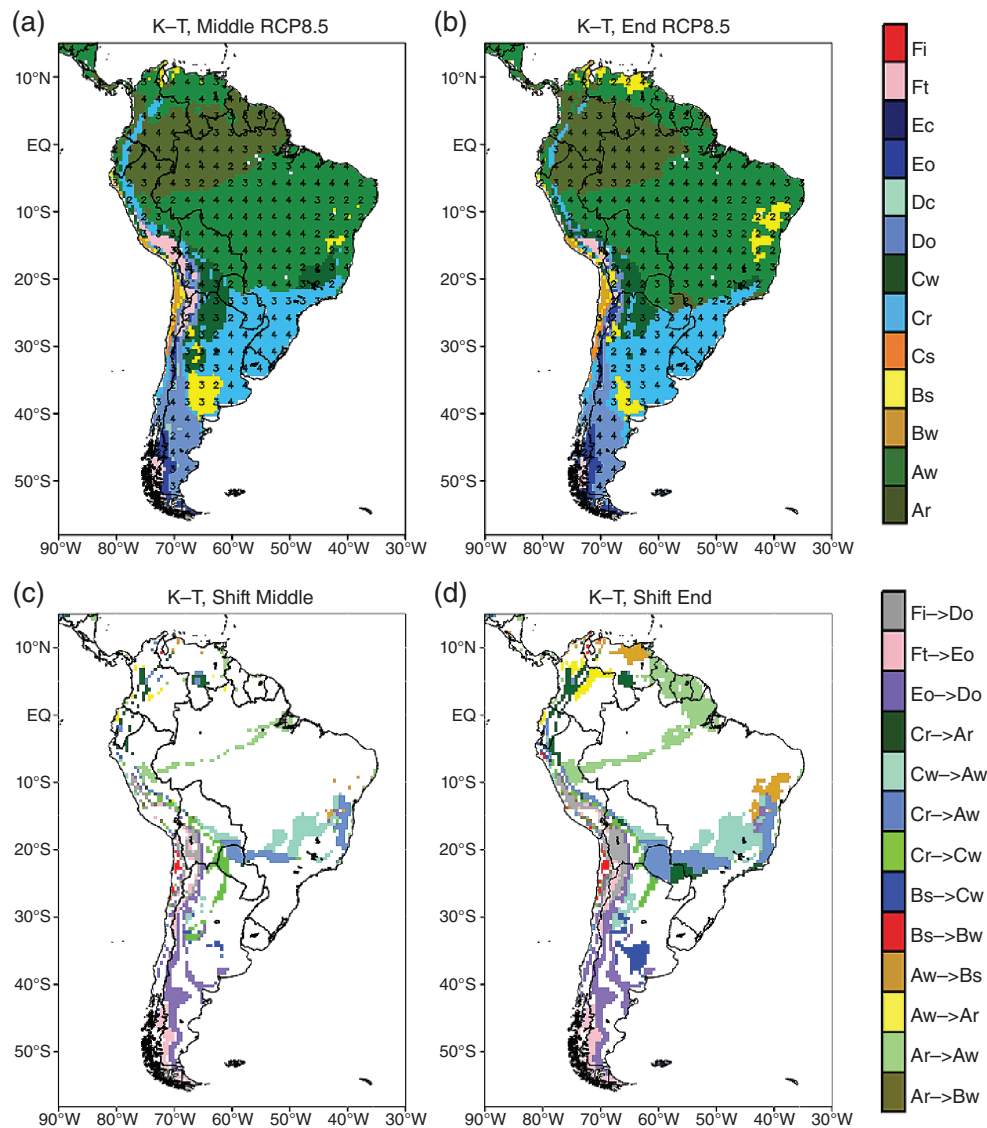


Figure 3. Köppen–Trewartha (K–T) climate types over SA calculated from RegCM4 mean ensemble for (a) middle (2035–2060) and (b) end (2075–2100) of the 21st century. Projected major K–T climate types transitions for (c) middle (2035–2060) and (d) end (2075–2100) of the 21st century under RCP 8.5 scenario. The numbers in the panels (a) and (b) indicate how many members have the same climate types as the mean ensemble.

(c). However, over the Amazon and NO regions, the K–T climate distribution is maintained (Figure 2(a)). The NEB region is also affected by the increase of temperature, but the impact is lower. On the other hand, if the temperature is maintained constant (Figures 4(b) and (d)) many projected transitions are reproduced over the tropical region while in the mountainous regions and south of SA the impact is lower. In North SA, AMZ, and North Brazil regions the decrease of precipitation causes a reduction in the tropical forest (Ar). In the NEB the reduction of precipitation and the increase of temperature provoke an increase of the aridity showing that both the factors are important for the arid zones in the tropical SA (figure not shown). In the Southeast and South SA, the increase of temperature causes a transition to more temperate climates.

To address the uncertainty in the projections numbers in the panel of Figures 2(b), 3(a) and (b) indicate

how many members have the same climate types as in the mean ensemble. As can be seen, the most part corresponds to 4 and 3 members of the RCM. This provides a more robust message of the changes identified. In general, the members show a positive bias of precipitation over NEB as result of an incorrect representation of the sea surface temperature in the tropical Atlantic both in present and future climates. Over the AMZ a negative anomaly of precipitation is noted.

The changes in the K–T climates are in general larger at the end of 21st century (Figure 2(d)). The most notable change is the increase of the aridity in NEB where the region of Bs (dry semiarid climate) is expanded compared to that in the mid-21st century. Other changes are seen in the Amazon, North Brazil, and north of Southeast Brazil. A larger increase of Aw (tropical wet-dry) and a retreat of Ar (tropical humid) are found in Amazon and North Brazil

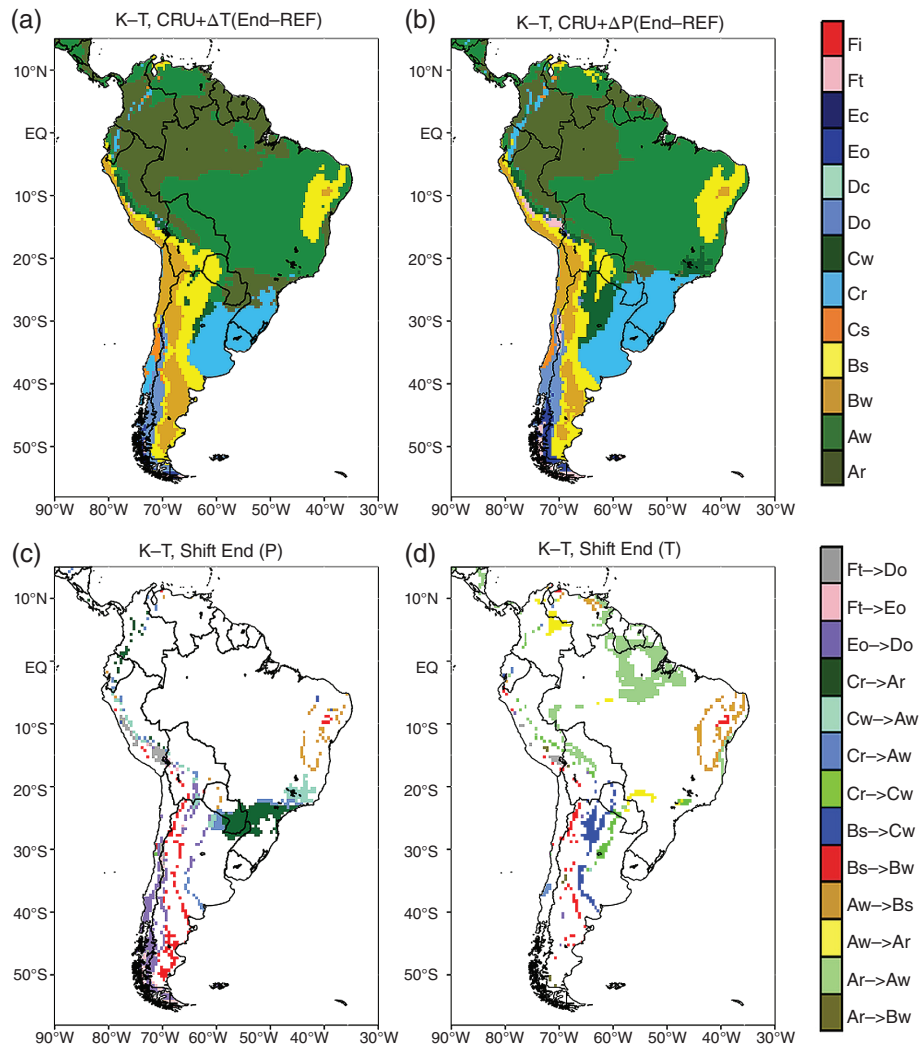


Figure 4. Same as Figure 2(d) (2e), but with trends of (a) [(c)] precipitation or (b) [(d)] temperature, removed.

compared to the mid-21st century. In the north of Southeast Brazil, the increase of Aw is also larger. In general, the changes are in agreement with those obtained from other RCMs (Gallardo *et al.*, 2016) and AOGCMs (Feng *et al.*, 2014) projections using SRES/CMIP5 scenarios, which also show transitions to drier climates over most of SA, mainly over Brazil.

The simulated changes in area (% of grid points on land) of the K–T types in the regions of SA showed in Figure 1 for the middle and end of the 21st century are given in Table S2. The changes are larger at the end of 21st century. The highest changes occur in the North Brazil, Amazon, and South Brazil: the coverage of Ar decreases by 21.3 and 13.3% at the end of the 21st century in North Brazil and Amazon, respectively; on the other hand, Aw area extends 21.3 and 13.5% in these regions. In the South Brazil, a great increase of Ar (35.6%) and reduction of Cr (32.9%) are noted at the end of the 21st century.

Figures 2(e) and (f) show the projected changes in K–T future climate transitions over SA for the middle and end 21st century. As can be seen, in the Andes, North of Argentina, South Brazil, and South of SA there

is a change to warm and wet climates while in the north of SA and NEB the projection is to a drier climate in future. In North Brazil and Amazon, there is a transition from a humid climate to a summer-wet climate. As can be noted the project changes in K–T climate types at the end of the 21st century are strongest.

4. Summary and conclusions

In this paper, the change of the biomes distribution over SA in the 21st century under the RCP 8.5 scenario is investigated using a mean ensemble of RegCM4 simulations. For this purpose, the K–T climate classification is used. The delta method is used as bias-correction of projections. The results showed that changes occur over SA already in the mid-21st century, and they are higher at the end of 21st century. Particularly over Brazil, notable changes of the K–T climate types are found in NEB, North Brazil, Amazon and Southeast Brazil. Over NEB the tropical wet-dry climate (Aw), is replaced by a drier climate (Bs), indicating the replacement of savanna by steppe. Ar decreases and Aw increases over North Brazil and Amazon, suggesting the substitution

of the rainforest by savanna. A retreat of subtropical humid climate (Cr) replaced by tropical wet-dry climate (Aw) is found in the Southeast Brazil, indicating the change of longleaf trees by savanna. Other changes can also be seen in Paraguay, Argentina, and the eastern SA. Cr decreases replaced by Ar over Paraguay. An increase of Cw and decrease of Cr are found in Argentina. At the western SA, Bs increases in Bolivia and in the west coast, a retreat of Eo and an increase of Do and Bw occurs. In general, in the Andes, north of Argentina, South Brazil, and South of SA there is a change to warm and wet climate while in the north of SA and NEB the change is to a dryer climate. In North Brazil and Amazon, there is a transition from a humid climate to a summer-wet climate.

The dominant factor for projected K–T climate type transitions in middle latitudes is the temperature changes while in the tropical region (AMZ) precipitation changes are the primary driver; for mountainous and arid regions both the factors are important.

In general, the changes in the biomes projected by the mean ensemble RegCM4 simulations agree with what is expected for future climate because of a dryer climate. These changes are already occurring mainly in Brazil, such as an increase of the aridity in NEB, reduction of forest in the coast and replacement of forest by savanna in the North Brazil and Amazon as a result of the changes in climate and landuse.

Although the results presented above were obtained through the mean ensemble of RegCM4 simulations with different physics configurations, driven at the lateral boundaries from various AOGCMs, some drawbacks (caveats) must be considered. The simulations did not take into account the change in vegetation due to climate conditions as well as the landuse alterations, mainly in the region of Amazon. Thus the inclusion of land surface parameterization with dynamic vegetation, biochemical cycle and the inclusion of deforestation scenarios could reduce the uncertainties due to these factors. This is subject to future studies.

Acknowledgements

Thanks are due to Dr. Gao and the ICTP for providing the K–T code and the CREMA dataset, respectively. The authors are also thankful to Dr. Rosmeri daRocha for a critical review of this manuscript, and to the anonymous reviewers for the useful comments to improve the article.

Supporting information

The following supporting information is available:

Figure S1. Same as Figure 2, but for UDEL observations.

Table S1. Descriptions of RegCM4 simulations forced by HadGEM2 (CERegHad and BGRegHad), MPI (CERegMPI) and GFDL (CERegGFDL) AOGCMs. The CE and BG indicate, respectively, that RegCM4 simulations used CLM-Emanuel and BATS-Grell schemes.

Table S2. Simulated changes (%) of K–T climate types over the regions of Figure 1 for the middle and end (in parentheses) of the 21st century.

References

- Belda M, Holtanová E, Kalvová J, Halenka T. 2016. Global warming-induced changes in climate zones based on CMIP5 projections. *Climate Research* **71**: 17–31.
- Boberg F, Christensen JH. 2012. Overestimation of Mediterranean summer temperature projections due to model deficiencies. *Nature Climate Change* **2**: 433–436.
- Castro M, Gallardo C, Jylha K, Tuomenvirta H. 2007. The use of a climate-type classification for assessing climate change effects in Europe from an ensemble of nine regional climate models. *Climatic Change* **81**: 329–341.
- Chan D, QG W, Jiang G, Dai XL. 2016. Projected shifts in Köppen climate zones over China and their temporal evolution in CMIP5 multi-model simulations. *Advances in Atmospheric Sciences* **33**: 283–293. <https://doi.org/10.1007/s00376-015-5077-8>.
- Christensen JH, Boberg F. 2012. Temperature dependent climate projection deficiencies in CMIP5 models. *Geophysical Research Letters* **39**: L24705. <https://doi.org/10.1029/2012GL053650>.
- Coppola E, Giorgi F, Raffaele F, Fuentes-Franco R, Giuliani G, Llopart-Pereira M, Mangain A, Mariotti L, Diro GT, Torma C. 2014. Present and future climatologies in the phase I CREMA experiment. *Climatic Change* **125**: 23–38. <https://doi.org/10.1007/s10584-014-1137-9>.
- Feng S, Hu Q, Huang W, Ho CH, Li R, Tang Z. 2014. Projected climate regime shift under future global warming from multi-model, multi-scenario CMIP5 simulations. *Global and Planetary Change* **112**: 41–52.
- Gao X, Giorgi F. 2008. Increased aridity in the Mediterranean region under greenhouse gas forcing estimated from high resolution simulations with a regional climate model. *Global and Planetary Change* **62**: 195–209.
- Gallardo C, Gil V, Hagel E, Tejada C, Castro M. 2013. Assessment of climate change in Europe from an ensemble of regional climate models by the use of Köppen–Trewartha classification. *International Journal of Climatology* **33**: 2157–2166.
- Gallardo C, Gil V, Tejada C, Sánchez E, Gaertner MA. 2016. Köppen–Trewartha classification used to assess climate changes simulated by a regional climate model ensemble over South America. *Climate Research* **68**: 137–149.
- Garreaud RD, Vuille M, Compagnucci R, Marengo J. 2009. Present-day South American climate. *Paleogeography, Palaeoclimatology, Palaeoecology* **281**: 180–195.
- Giorgi F. 2014. Introduction to the special issue: the phase I CORDEX RegCM4 hyper-matrix (CREMA) experiment. *Climatic Change* **125**: 1–5.
- Giorgi F, Coppola E, Solmon F, Mariotti L, Sylla MB, Bi X, Elguindi N, Diro GT, Nair V, Giuliani G, Turuncoglu UU, Cozzini S, Güttler I, O'Brien TA, Tawfik AB, Shalaby A, Zakey AS, Steiner AL, Stordal F, Sloan LC, Brankovic C. 2012. RegCM4: Model description and preliminary tests over multiple CORDEX domains. *Climate Research* **52**: 7–29.
- Giorgi F, Jones C, Asrar G. 2009. Addressing climate information needs at the regional level: the CORDEX framework. *WMO Bulletin* **58**: 175–183.
- Harris I, Jones PD, Osborn TJ, Lister DH. 2014. Updated high-resolution grids of monthly climatic observations – the CRU TS3.10 dataset. *International Journal of Climatology* **34**: 623–642.
- Lohmann U, Sausen R, Bengtsson L, Cubasch U, Perlwitz J, Roeckner E. 1993. The Köppen climate classification as a diagnostic tool for general circulation models. *Climate Research* **3**: 177–193.
- Mahlstein I, Daniel JS, Solomon S. 2013. Pace of shifts in climate regions increases with global temperature. *Nature Climate Change* **3**: 739–743.
- Matsuura K, Willmott CJ. 2011. Terrestrial air temperature: 1901–2014 gridded monthly time series (Version 4.01). <http://www.>

- esrl.noaa.gov/psd/data/gridded/data.UDeI_AirT_Precip.html. (accessed 3 April 2017).
- Nakićenović N, Alcamo J, Davis G, et al. 2000. *IPCC Special Report on Emissions Scenarios*. Cambridge University Press: Cambridge, UK and New York, NY.
- Piani C, Weedon GP, Best M, Gomes SM, Viterbo P, Hagemann S, Haerter JO. 2010. Statistical bias correction of global simulated daily precipitation and temperature for the application of hydrological models. *Journal of Hydrology* **395**: 199–215.
- Solman S, Sanchez E, Samuelson P, daRocha RP, Li L, Marengo J, Pessacg NL, Remedio ARC, Chou SC, Berbery H, Le Treut H, de Castro M, Jacob D. 2013. Evaluation of an ensemble of regional climate model simulations over South America driven by the ERA-Interim reanalysis: model performance and uncertainties. *Climate Dynamics* **41**: 1139–1157.
- Solman S. 2016. Systematic temperature and precipitation biases in the CLARIS-LPB ensemble simulations over South America and possible implications for climate projections. *Climate Research* **68**: 117–136.
- Teichmann C, Eggert B, Elizalde A, Haensler A, Jacob D, Kumar P, Moseley C, Pfeifer S, Rechid D, Remedio AR, Ries H, Petersen J, Preuschmann S, Raub T, Saeed F, Sieck K, Weber T. 2013. How Does a Regional Climate Model Modify the Projected Climate Change Signal of the Driving GCM: A Study over Different CORDEX Regions Using REMO. *Atmosphere* **4**: 214–236.
- Trewartha GT, Horn LH. 1980. *An introduction to climate*, 5th ed. McGraw-Hill: New York, NY.